Food Chemistry: X 26 (2025) 102292

Contents lists available at ScienceDirect

Food Chemistry: X

journal homepage: www.sciencedirect.com/journal/food-chemistry-x

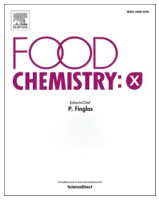

Comparison between Indian and commercial chamomile essential oils: Chemical compositions, antioxidant activities and preventive effect on oxidation of Asian seabass visceral depot fat oil

Birinchi Bora [a], Tao Yin [b], Bin Zhang [c], Can Okan Altan [d], Soottawat Benjakul [a,e,*]

[a] International Center of Excellence in Seafood Science and Innovation (ICE-SSI), Faculty of Agro-Industry, Prince of Songkla University, Hat Yai, Songkhla, 90110, Thailand
[b] College of Food Science and Technology, Huazhong Agricultural University, Wuhan, Hubei Province, 430070, PR China
[c] College of Food Science and Pharmacy, Zhejiang Ocean University, Zhoushan, Zhejiang, China
[d] Department of Seafood Processing Technology, Faculty of Fisheries, Sinop University, Sinop, 57000, Türkiye
[e] b BioNanocomposite Research Center, Department of Food and Nutrition, Kyung Hee University, 26 Kyungheedae-ro, Dongdaemun-gu, Seoul 02447, Republic of Korea

ARTICLE INFO

Keywords:
Chamomile essential oil
Seabass visceral depot fat
Lipid oxidation
Polyunsaturated fatty acid
Oxidative stability
Fish oil

ABSTRACT

Antioxidant properties of indigenous Indian (ICO) and commercial (CCO) chamomile essential oils (EOs) and their application in preventing lipid oxidation of fish oil were investigated. Solid-phase micro-extraction gas chromatography–mass spectrometry (SPME-GCMS) revealed dominant compounds to be α-bisabolol and chamazulene in ICO, while α-farnesene and δ-cadinene in CCO. Both EOs exhibited similar 2,2-diphenyl-1-picrylhydrazyl (DPPH) radical scavenging activity and oxygen radical absorbance capacity (ORAC) values but ICO showed superior effect in β-carotene/linoleic system. When applied in Asian seabass visceral depot fat oil (SVDFO), ICO (400 mg/L) significantly reduced peroxide values after 15 days (30°C) and slightly lowered thiobarbituric acid reactive substances and anisidine values. ICO (400 mg/L) showed comparable efficacy in preventing the oxidation of polyunsaturated fatty acids (PUFAs) to 200 mg/L butylated hydroxytoluene (BHT) within 0–12 days. Fourier Transform Infrared (FTIR) analysis confirmed preservation of PUFA double bonds by ICO. Therefore, chamomile EOs, especially ICO, could prevent lipid peroxidation in PUFA-rich oils.

1. Introduction

Medicinal and aromatic plants (MAPs) are essential traditional medicines and are also used in food, pharmaceuticals, cosmetics, and perfumes. The World Health Organization estimates that about 80 % of people worldwide use herbal products in some ways or the other (W.H.O., 2021). The global herbal market is estimated at over USD 100 billion and is growing by 15 % annually (Khan & Ahmad, 2019). The valuable components of these plants, like essential oils (EOs) and extracts, which make up to 0.5 % to 8 % of the plant's total mass, are rich in high value bioactive compounds which can potentially be used in food and pharmaceutical industries (Saha & Basak, 2020). EOs are volatile aromatic compounds produced in plant metabolism, mainly terpenoids, including monoterpenes and sesquiterpenes (Gölükcü et al., 2024). Generally, EO composition is influenced by several factors such as cultivar, harvesting time, isolation technique, etc. (Bozova et al., 2024).

German Chamomile (*Matricaria chamomilla* L.) is a MAP, originated from Southern and Eastern Europe. During the last century, it has spread throughout Asia (El Mihyaoui et al., 2022). Components from natural resources available in each region have gained interest, from which various types of value-added products can be exploited (Yarnpakdee et al., 2015). Chamomile flowers have been used for EO extraction, mainly via hydrodistillation and the yield varies from 0.24 % to 1.90 % based on numerous factors (Pathania et al., 2024; Rathore & Kumar, 2021), leaving behind other valuable byproducts such as floral distillates (hydrosols), water-soluble filtrates, and spent biomass which can also be exploited as the sources of polyphenols and other bioactive constituents. Chamomile EO consists of several bioactive compounds, especially α-bisabolol and chamazulene (Tsivelika et al., 2018). Moreover, German chamomile EO possesses numerous pharmacological and biological activities, e.g. anti-inflammatory, antioxidant, anti-microbial, anti-septic, anti-ulcerogenic, sedative and wound healing activities, etc.

* Corresponding author at: International Center of Excellence in Seafood Science and Innovation (ICE-SSI), Faculty of Agro-Industry, Prince of Songkla University, Hat Yai, Songkhla 90110, Thailand.
E-mail address: soottawat.b@psu.ac.th (S. Benjakul).

https://doi.org/10.1016/j.fochx.2025.102292
Received 30 December 2024; Received in revised form 31 January 2025; Accepted 16 February 2025
Available online 20 February 2025

(Chauhan et al., 2022). EOs can be used in food industry with different purposes such as used as antimicrobial and antioxidative agents in salad cream or functional dairy product such as cottage cheese (Caleja et al., 2015; Lertchirakarn & Muangrat, 2023). These EOs can be better exploited as natural antioxidants agents, especially in edible oils due to their strong bioactivities and compatibility with oils. However, antioxidant compounds in EO from different Chamomile flowers can be varied, depending on geographic location, climate, soil, etc. (Piri et al., 2019).

Fish oil extracted from the processing leftover such as head, internal organs as well as depot fat has been considered to be rich in n-3 PUFAs (Benjakul et al., 2019; Rajasekaran et al., 2024), especially docosahexaenoic acid (DHA) and eicosapentaenoic acid (EPA) (Miyashita et al., 2018). n-3 PUFAs have contributed to the health benefits, involving the prevention of cardiovascular diseases, inflammation and cancer (Dale et al., 2019; Lauritzen, 2021).

Nowadays, there is a rapidly growing demand for fish oil supplements in the global market (Alfio et al., 2021). As per IFFO (2022), 53 % of total fish oil produced is extracted from the byproducts obtained from the fish processing industries. In the year 2021, it was reported that among fish oil produced, 74 % was utilized in aquaculture, 16 % for human consumption and 10 % for pet foods and biofuel (Ababouch & Vannuccini, 2024). Various methods are used for fish oil extraction such as wet and dry rendering, enzymatic hydrolysis, solvent and supercritical-fluid extraction, and mechanical pressing (Sae-leaw & Benjakul, 2017; Saleh et al., 2022). The wet rendering process is the most employed technique for fish oil recovery. It includes size reduction, heating, pressing, separation, degumming, and further refining, etc. (Ahmmed et al., 2020; Saleh et al., 2022).

Asian seabass (*Lates calcarifer*) is a popularly cultured species associated with fast growth rate and tolerance to varying environments. This species is naturally found and widely cultivated in Southeast Asian countries such as Thailand, Malaysia, Indonesia and Singapore ((Wong et al., 2023; Yue et al., 2022). During its evisceration, depot fat along with the viscera attached to the belly cavity can be collected and utilized for the production of prime quality fish oil (Sae-leaw & Benjakul, 2017). Oil derived from depot fat is rich in PUFAs (Patil & Benjakul, 2019). Therefore, the oil is very prone to oxidative deterioration. Lipid oxidation negatively affects the taste, aroma, color and nutritive value of fish oil associated with quality deterioration (Q. Li et al., 2023; Miyashita et al., 2018). Hence, prevention of lipid oxidation is very vital for fish oil preservation.

In general, synthetic antioxidants or α-tocopherol have been widely used to prevent lipid oxidation in fish oil. However, synthetic additives have been of safety concern. EOs, especially from Chamomile flower, could serve as an alternative potential antioxidant in fish oil, due to its compatibility and safety. However, a little information on antioxidant activities in varying assays and the application of both ICO and CCO in fish oil has been documented. Therefore, this study aimed to provide the insights into chemical compositions and antioxidant activities of Chamomile EOs from different two origins. The preventive effect toward oxidation of fish oil was also monitored during the extended storage.

2. Materials and methods

2.1. Flower collection and EO extraction

The fresh capitula of wild German Chamomile flowers were harvested between March 2024 and April 2024 from Palampur, Himachal Pradesh, India. The flowers were plucked carefully and washed using flowing tap water to remove the soil and air-dried with the aid of a fan for 12 h. Dried flowers were then kept in an airtight plastic box at 4 °C until use.

For EO extraction, fresh flowers (3 kg) were transferred into a 5-L round bottom flask (RBF) and added with 2 L of distilled water. The mixture was placed on a heating mantle and heated up to 95 °C. Hydrodistillation was done for 3 h using a Clevenger apparatus. EO was collected and anhydrous sodium sulfate (500 mg) was mixed to eliminate residual moisture in the extracted EO. The EO yield was expressed as mL/g dried flower. The obtained EO was stored in an airtight glass vial under refrigerated condition (4 °C) for further use or analyses (Pathania et al., 2024).

2.2. Collection of Asian seabass visceral depot fat (SVDF) and extraction of SVDF oil (SVDFO)

The entire viscera of the freshly caught Asian seabass and depot fat from the belly cavity were collected and bought from a local market in Hat Yai, Thailand and delivered in ice (1:2 w/w) within 30 min to the laboratory. Depot fat was collected and size reduction was done using a knife before blending with the aid of a blender (National, MXT2GN, Taipei, Taiwan). The extraction of SVDFO was done under a vacuum in a round bottom flask connected to a rotary evaporator (N1000, EYELA, Tokyo Rikakikai Co., Ltd., Tokyo, Japan). The prepared sample (100 g) was heated and continuously swirled for 30 min at 50 °C. After the heating process, the resultant mixtures were centrifuged using a refrigerated centrifuge (CR22N, Hitachi, Hitachi Koki Co., Ltd. (10,000 g, 4 °C) for 20 min to remove the residual tissue. The oil was then collected, placed in amber glass bottle and tightly capped before storing at 4 °C for further study (Sae-leaw & Benjakul, 2017).

2.3. SPME-GCMS of Chamomile EOs

SPME-GCMS was employed for the identification of volatile compounds in ICO and CCO (Sae-leaw et al., 2016). The SPME fiber (SU57343Uc) was conditioned at 250 °C for 15 min before being exposed to the headspace to absorb the tested volatile compounds. After being desorbed, Agilent 5190–2294 gas chromatography (GC) coupled with a mass-selective detector equipped with a split injector and a triple quadrupole mass detector was employed for the GC–MS analysis. Compounds were separated using an Agilent 19091S—433I column (30 × 0.25 mm ID, 0.25 μm film thickness). The quadrupole mass spectrometer was configured to electron ionization mode with a source temperature of 230 °C. Initially, full scan mode data was collected to identify acceptable masses for later capture in scan mode (Mass range: 29–500 amu and scan rate: 0.770 s/scan).

2.4. Antioxidant activity of Chamomile EOs

2.4.1. DPPH radical scavenging activity (DPPH-RSA)

DPPH-RSA of both EOs was determined as described by Ahmad et al. (2024). EOs were diluted in 99.99 % dimethyl sulfoxide (DMSO) to obtain the concentration of 1 mg/mL. Thereafter, 150 μL of 0.15 mmol/L DPPH solution was mixed with an equal volume of EOs solution in a 96-well microtiter plate. The absorbance at 517 nm was measured every 5 min up to 60 min of incubation. DMSO was utilized to replace DPPH solution and considered as the sample blank. A standard curve of Trolox (10–60 μM) was prepared. The activity was computed after the sample blank subtraction and reported as mmol Trolox equivalents (TE)/g EO.

2.4.2. Oxygen radical absorbance capacity (ORAC)

ORAC of both EOs was also tested (Sae-leaw et al., 2016). After reaction, the fluorescence intensity was monitored every 5 min for 150 min. The excitation and emission wavelengths used were 485 and 535 nm respectively. The area under the fluorescence decay curve (AUC) was computed by the normalized curves using the following equation:

$$AUC = 0.5 + \frac{f2}{f1} + \frac{f3}{f1} + \frac{f4}{f1} \ldots\ldots\ldots + 0.5\frac{fn}{f1}$$

where, f1 = fluorescence at the initiation of the reaction and fn = fluorescence at the end of the reaction. The net AUC was calculated by subtracting the blank AUC from that of the sample or standard AUC. Trolox (0–100 μM) was used as a standard and ORAC was reported in

μmol TE/g EO.

2.4.3. β -carotene/linoleic acid bleaching assay

Firstly, an emulsion containing β-carotene, linoleic acid and Tween 40 (5 mL) was mixed with EOs dissolved in DMSO (10 μL) and the absorbance at 470 nm (A_{470}) was read against the blank (emulsion with no β-carotene). Reaction was carried out at 50 °C and the oxidation was measured spectrometrically by measuring A_{470} up to 120 min. Control was prepared using water instead of EOs. The antioxidant activity was indicated by the retarded bleaching rate of system (Sengupta et al., 2015). The bleaching retardation efficiency (BRE) was calculated by the following equation:

BRE (%) = (1 - (A_0-A_{120})/A_0) x 100.

where BRE = Bleaching retardation efficiency; A_0 = Absorbance at time 0 min; A_{120} = Absorbance at time 120 min

2.5. Effect of EOs at various levels on oxidative stability of SVDFO during the storage

2.5.1. Sample preparation

SVDFO was filled in a beaker. ICO and CCO were added to SVDFO and mixed well to obtain the final concentrations of 200 and 400 mg/L. BHT was added to SVDFO at 200 mg/L and used as a positive control. The samples were mixed gradually using a stirrer for 30 min with the aid of a magnetic bar. Finally, each sample (80 mL) was filled in a 100 mL amber bottle, keeping a headspace of 2 cm height from the top. A control sample without any antioxidants was also prepared. All the bottles were kept uncapped at 30 °C in an incubator. The experiment was conducted for 15 days due to extremely high susceptibility to lipid oxidation of SVDFO. The samples from each treatment were collected every 3 days up to 15 days for analyses. Nonetheless, fatty acid profile and FTIR spectra were determined on days 0 and 15.

2.5.2. Analyses

2.5.2.1. Peroxide value (PV). PV measurement of SVDFO was conducted using the ferric thiocyanate method as reported by Takeungwongtrakul and Benjakul (2013). The SVDFO samples (50 μL) was combined with 2.5 mL of chloroform/methanol (2:1, v/v), followed by addition of 50 μL of 30 % ammonium thiocyanate (w/v) and 50 μL of 20 mM ferrous chloride solution in 3.5 % HCl (w/v). After 20 min, the absorbance of the colored solution was measured at 500 nm with a spectrophotometer (Shimadzu UV-1800, Kyoto, Japan). The blank was produced similarly, using distilled water instead of ferrous chloride. A standard curve of cumene hydroperoxide (0–2 mg/L) was prepared. PV was computed from the standard curve and reported as mg cumene hydroperoxide/100 g SVDFO after blank subtraction.

2.5.2.2. Thiobarbituric acid reactive substances (TBARS). TBARS values of SVDFO samples were determined using thiobarbituric acid reagent (Pudtikajorn et al., 2022). The oil sample (0.5 mL) was combined with 2.5 mL of a solution containing 0.375 % thiobarbituric acid (w/v), 15 % trichloroacetic acid (w/v), and 0.25 M HCl. The mixture was heated in boiling water (95–100 °C) for 10 min to obtain a pink color and then cooled with running tap water. The solution was then centrifuged at 3600 xg at 25 °C for 20 min using a Beckman-Coulter Avanti J-E Centrifuge (Fullerton, CA, USA). The absorbance of the supernatant was measured at 532 nm with a spectrophotometer. TBARS values were computed from the standard curve of 1,1,3,3-tetramethoxypropane (0–6 mg/L) and reported as malonaldehyde meq/100 g SVDFO.

2.5.2.3. p-Anisidine value (AnV). SVDFO samples (0.3 mL) were dissolved in 10 mL of isooctane (S1). Then, 0.5 mL of anisidine reagent (0.5 % ρ-anisidine in acetic acid) was added (S2). The solution was kept in the dark for 10 min before measuring its absorbance at 350 nm using a spectrophotometer. A_1 and A_2 were recorded, respectively. Two blanks included the blank prepared with pure isooctane (B1) and the blank prepared using pure isooctane added with ρ-anisidine (B2). AnV was calculated by using the following equation:

p-AnV = 10 x (1.2 x (A_{S2}-A_{B2}) – (A_{S1}-A_{B1})).

2.5.2.4. Conjugated diene (CD). CD of SVDFO was examined as per the IUPAC method (Pudtikajorn & Benjakul, 2020). SVDFO samples (0.1 g) were mixed with 100 mL of isooctane. The absorbance at 234 nm (A_{234}), representing the CD formed, was read. The CD values were computed as follows:

CD = A_{234}/ Weight of SVDFO (g) × Cell path length (cm).

2.5.2.5. Fatty acid profile. Fatty acid methyl esters (FAMEs) of SVDFO were firstly prepared (Raju et al., 2021) and FAMEs were injected into an Agilent 7890B gas chromatograph with a flame ionization detector (GC-FID; Santa Clara, CA, USA). Fatty acid peaks were identified by comparing with the retention times of standards and the content of fatty acids was computed and reported as g/ 100 g sample.

2.5.2.6. Fourier transform infrared (FTIR) spectra. FTIR spectra were determined with a Bruker Vertex 70 FTIR spectrometer (Bruker Co., Ettlingen, Germany). SVDFO (200 μL) was placed in a crystal cell and placed in the FTIR spectrometer. The middle infrared region (4000–400 cm^{-1}) with 32 scans was used and the resolution of 4 cm^{-1} was employed. Normalization of signal was done using the spectrum of a clean empty cell. For spectral analysis, OPUS 3.0 data collection software (Bruker Co. Billerica, MA, USA) was utilized (Pudtikajorn & Benjakul, 2020).

2.5.2.7. Color values. Colors of different samples were observed by measurement of CIE Lab values (L^* = lightness, a^* = redness and greenness, b^* = yellowness and blueness) using a Hunter Lab (Colorflex, Reston, VA, USA) (Pudtikajorn et al., 2022).

2.6. Statistical analyses

All the experiments and analyses were done in triplicate. The data were expressed as mean ± standard deviation. SPSS 28.0 (IBM Corporation, NY, USA) was employed to run an analysis of variance (ANOVA), and Duncan's multiple range test was utilized for comparing the mean values. P-value less than 0.05 ($p < 0.05$) was considered 'significant.'

3. Results and discussion

3.1. Chemical composition of Chamomile EOs

Chemical compositions, mainly volatile compounds, of both Indian (ICO) and commercial (CCO) Chamomile EOs were analyzed by SPME-GCMS as shown in Table 1. Twenty-five compounds involving monoterpenes, oxygenated monoterpenes, sesquiterpenes, oxygenated sesquiterpenes, etc. were found in both EOs (Table 1). The most abundant compounds detected in ICO were D-Limonene, γ-Terpinene, cis-β-Farnesene, α-Farnesene, δ-Cadinene and α-Bisabolol. CCO was abundant in γ-Terpinene, α-Farnesene and δ-Cadinene. Other studies also reported the prevalence of these compounds in Chamomile EOs (Pathania et al., 2024; Stanojevic et al., 2016). Compounds such as α-Bisabolol possessed antioxidant and antimicrobial potentials (Lim et al., 2021; Meeran et al., 2018). High levels of α-Bisabolol in ICO suggested its anti-inflammatory and skin-soothing properties (Barreto et al., 2016). Higher levels of δ-Cadinene and α-Farnesene present in the CCO plausibly contributed to its aroma and antioxidant activity (Y. Li et al., 2016). Chamazulene was detected in ICO but was not found in the CCO. This compound is a potent antioxidant and is able to reduce the oxidative stress of cells caused by reactive oxygen species (Gabbanini et al., 2024). Furthermore, another

Table 1
Volatile compounds in Indian and commercial Chamomile essential oils as analyzed by SPME-GCMS.

Compounds	Formula	ICO*	CCO*
3-Thujene	$C_{10}H_{16}$	39.20	ND
4(10)-Thujene	$C_{10}H_{16}$	217.53	603.70
2(10)-Pinene	$C_{10}H_{16}$	191.84	251.91
D-Limonene	$C_{10}H_{16}$	1929.99	ND
γ-Terpinene	$C_{10}H_{16}$	1138.20	1457.08
α-Terpinene	$C_{10}H_{16}$	620.58	ND
Artemisia alcohol	$C_{10}H_{18}O$	61.91	ND
Geraniol	$C_{10}H_{18}O$	35.89	133.13
α-Gurjunene	$C_{15}H_{24}$	13.42	308.66
(*E*)-β-Farnesene	$C_{15}H_{24}$	72.85	ND
cis-β-Farnesene	$C_{15}H_{24}$	19484.15	96.66
β-Selinene	$C_{15}H_{24}$	406.35	432.52
α-Farnesene	$C_{15}H_{24}$	3860.76	6099.04
δ-Cadinene	$C_{15}H_{24}$	3038.58	4941.25
Naphthalene, 1,2,3,4,4a,7-hexahydro-1,6-dimethyl-4-(1-methylethyl)-	$C_{15}H_{24}$	184.76	352.54
α-Patchoulene	$C_{15}H_{24}$	133.01	ND
T-Cadinol	$C_{15}H_{26}O$	533.18	ND
α-Bisabolol	$C_{15}H_{26}O$	7186.64	19.72
trans-Farnesol	$C_{15}H_{26}O$	23.14	ND
Chamazulene	$C_{14}H_{16}$	841.19	ND
Farnesol, acetate	$C_{17}H_{28}O_2$	2.60	4.71
(Z)-2-(Hexa-2,4-diyn-1-ylidene)-1,6-dioxaspiro[4.4]non-3-ene	$C_{13}H_{12}O_2$	19.11	ND
Thiogeraniol	$C_{10}H_{18}S$	21.27	ND
(E)-2-(Hepta-2,4-diyn-1-ylidene)-1,6-dioxaspiro[4.4]non-3-ene	$C_{14}H_{14}O_2$	16.54	ND
m-Camphorene	$C_{20}H_{32}$	3.09	4.56

ICO: Indian Chamomile EO, CCO: Commercial Chamomile EO.
ND- not detected.
*Values are represented as the abundance (x 10^6).

bioactive compound detected in the ICO was D-Limonene, which had the potential to neutralize free radicals (Anandakumar et al., 2021). Overall, the compositions or volatile compounds in both EO samples were different, which might be due to the genotypes, environmental factors, location, mode of growing, planting time, processing techniques, etc. (Piri et al., 2019). Factors such as soil quality, climate and geography, etc. influence the EO chemical composition as well as its quality (Yadav et al., 2022). Therefore, the antioxidant and other bioactivities of the EOs were governed by the presence of various terpenes and other aromatic compounds, which could be varied in type and content.

3.2. Antioxidant activities of Chamomile EOs

Antioxidant activities of ICO and CCO samples are illustrated in Fig. 1. Chamomile EOs and different extracts have been used worldwide as excellent antioxidants (Pathania et al., 2024; Zengin et al., 2023). Radical scavenging activity (RSA) is one of the crucial mechanisms for terminating the propagation of lipid oxidation (Valgimigli, 2023). DPPH$^{\bullet}$ (radical) can accept hydrogen atoms, forming a stable DPPH-H. This stable diamagnetic DPPH-H radical formation changes the color of the reaction solution from purple to yellow, reflecting the radical scavenging capacity of the sample (Al-Dabbagh et al., 2019). DPPH-RSA of ICO was 13.06 ± 0.01 mmol TE/g and that of CCO was 13.91 ± 0.02 mmol TE/g of oil. The results suggested that Chamomile EOs possessed a high antioxidant activity. These findings were in tandem with other previous reports (Stanojevic et al., 2016; Tsivelika et al., 2018). ORAC was also used for the determination the ability of EO in scavenging peroxyl radical (Amigo-Benavent et al., 2021). ORAC indicates the potential of antioxidants present in samples to break the radical chain. A non-fluorescent product is generated after the reaction between the peroxyl radical and a fluorescent probe, which can be quantified by fluorescence intensity over time (Singh et al., 2019). ORAC is based on the principle of decrease in the intensity of fluorescent molecules, e.g. fluorescein under the constant generation and reaction of peroxyl

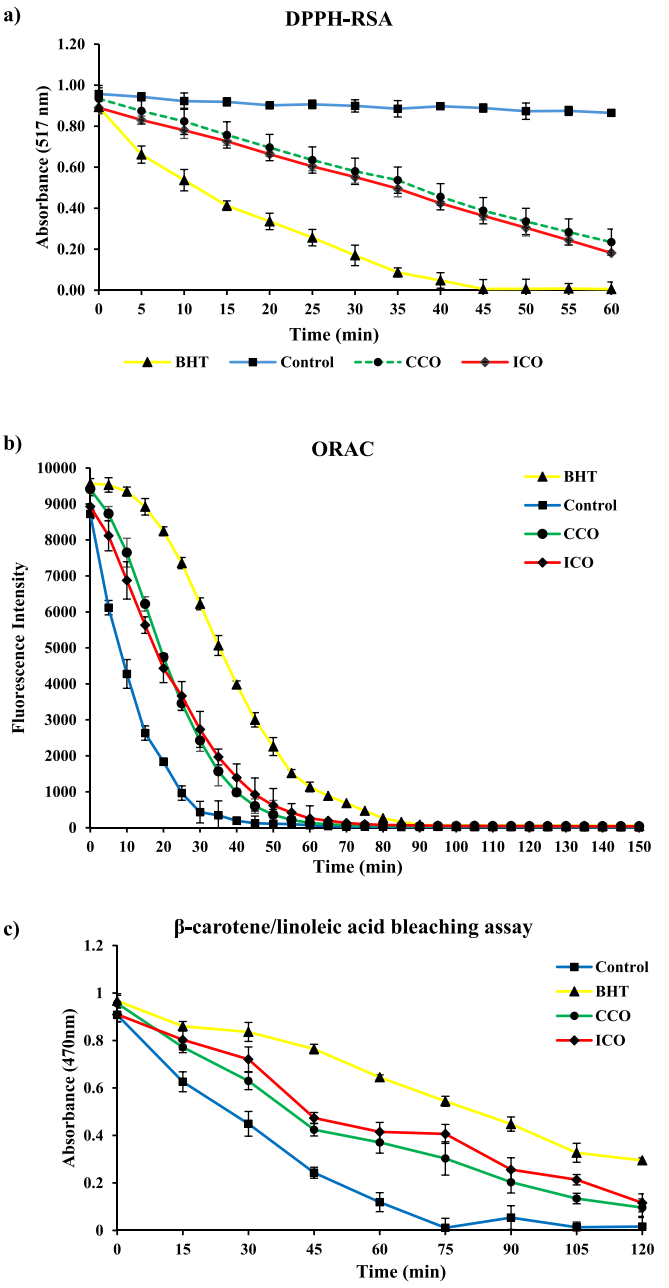

Fig. 1. Antioxidant activities of Indian and commercial German Chamomile essential oils using DPPH-RSA (a) ORAC (b) and β-carotene/linoleic acid bleaching (c) assays. Bars represent the standard deviation (n = 3).

radicals, which are formed in an aqueous buffer by thermal decomposition of 2,2-azobis (2-amidinopropane dihydrochloride) (Mittal et al., 2023). The control (without EOs or antioxidants) showed a rapid decrease in the fluorescence intensity. For ORAC, ICO (202.07 ± 0.03 μmol TE/g) showed a nearly similar value with CCO (199.95 ± 0.02 μmol TE/g), suggesting the similar peroxyl radical scavenging potential of both EOs. ORAC values of *Veronica saturejoides* EO were reported to be 255.10 ± 2.54 μmol TE/g for Prenj sample and 256.50 ± 5.73 μmol TE/g for Kamešnica sample (Nazlić et al., 2020).

Moreover, β-carotene/linoleic acid bleaching assay was employed to measure the antioxidant properties of the Chamomile EOs in comparison with BHT at 200 mg/L (Fig. 1c). The capacity of the EOs to retard the oxidation or discoloration of β-carotene present in a linoleic acid emulsion system was observed. Without antioxidant, the β-carotene molecules get oxidized and lose their double bond as the incubation time

upsurged. During this process, the characteristic orange color of β-carotene is lost which can be determined spectrophotometrically (Candido et al., 2022). Among the tested samples, after 120 min the system containing BHT showed the highest bleaching retardation efficiiency (BRE) of the β-carotene by 66.19 %, followed by ICO with 78.24 % and CCO by 85.60 %. The highest absorbance at 470 nm was retained by BHT followed by ICO and CCO at 0.30, 0.17 and 0.01 respectively, relative to the initial value after 120 min. No significant differences in A_{470} between systems added with CCO and ICO were found within the first 15 min ($p > 0.05$). This might be due to similar antioxidant activity to retard the oxidation of system at the initial state. However, with increasing incubation time, ICO showed the higher efficacy in retarding the oxidation of system. This was plausibly due to the higher antioxidant activity of ICO associated with higher potential antioxidant compounds. This was evidenced by the higher maintenance of β-carotene in the system (higher A_{470}). Different antioxidant compounds were found between both essential oils(Table 1). The antioxidant activity was similar to those reported by Amiri (2012) in the oils of *T. eriocalyx* (57.60 %), *T. kotschyanus* (69.20 %) and *T. daenensis subsp lancifolius* (88.40 %). Thus, ICO exhibited higher antioxidant activity than CCO assayed by the β-carotene/linoleic acid bleaching system.

3.3. Oxidative stability of SVDFO affected by Chamomile essential oil during storage

3.3.1. PV

PV is used for the determination of the initial lipid oxidation products such as hydroperoxides (Jacobsen et al., 2021). These lipid hydroperoxides are formed due to the oxidative reactions of PUFAs induced by singlet oxygen molecules or lipoxygenase (Zhang et al., 2021). PVs of SVDFO with varying treatments during 15 days are depicted in Fig. 2a**.** On day 0, PV ranged from 10.89 to 12.76 mg cumene hydroperoxide/100 g oil. PV upsurged with rising storage time until the end (15 days) ($p < 0.05$). This increasing trend indicated that the samples underwent lipid oxidation to a higher extent.

At the same storage time, SVDFO had the highest PV values, followed by the SVDFO+CCO (200), SVDFO+CCO (400), SVDFO+ICO (200), SVDFO+ICO (400) and SVDFO+BHT, respectively. ($p < 0.05$). Overall, the sample without any antioxidants (SVDFO) had higher formation of hydroperoxide during the storage period, whereas the sample added with BHT showed the least PV ($p < 0.05$). The lower PV value was obtained in the samples containing ICO (SVDFO+ICO) when compared to the samples containing CCO (SVDFO+CCO) when the same level was used. Overall, lower PV was attained in the sample added with higher levels of EOs (400 mg/L) ($p < 0.05$), especially for the sample incorporated with ICO. The presence of Chamomile EO, having a strong antioxidant property (Alahmady et al., 2024), might be related to the lowered production of hydroperoxides during the prolonged storage of fatty foods including SVDFO (Caleja et al., 2015). This was more likely due to the presence of antioxidants, especially α-bisabolol and chamazulene in the EOs (Capuzzo et al., 2014; Ramazani et al., 2022).

3.3.2. Conjugated diene value

Different CD values ($p < 0.05$) were obtained among the samples, particularly at the end of storage (Fig. 2b). CDs are primary products of lipid oxidation, which are generated when the double bonds in PUFA are converted into a conjugated diene structure (Huang & Ahn, 2019). Double bonds in PUFA are extremely susceptible to oxidation induced by radicals, in which 1,4-pentadiene structure undergoes changes where an H atom is easily abstracted from the structure by a hydroxyl radical. During the process, a double bond near the oxygen-deprived carbon attaches to another double bond and CDs are formed. The CD has a maximum absorbance of 234 nm and can be used for its spectrophotometric detection (Abeyrathne et al., 2021). On day 15, the CD values among the SVDFO samples ranged from 77.19 to 83.49. The trend was similar to the PV of the samples, where SVDFO has the highest value ($p < 0.05$), followed by the other samples viz. SVDFO+CCO (200), SVDFO+CCO (400), SVDFO+ICO (200), and SVDFO+ICO (400). Nonetheless, the SVDFO+BHT sample had the lowest CD value of 77.19 ($p < 0.05$), when compared with the other lipid samples followed by the SVDFO+ICO (400) having CD value of 79.29. Hence, the results confirmed that ICO and CCO could be used to prevent the oxidation of SVDFO in a concentration dependent manner. This result coincided with PV (Fig. 2a).

3.3.3. Anisidine value (AnV)

AnV showed an increasing trend among the oil samples with prolonged storage as depicted in Fig. 3a. AnV is a parameter to determine the secondary non-volatile lipid oxidation products. After the decomposition of hydroperoxides, some non-volatile products like aldehydes, ketones, lactones, acids, alcohols, dienals, epoxide monomers, hydroxy components, etc. are generated (Miyazawa, 2021). These compounds, especially 2-alkenals and 2,4-alkadienals could react with *p*-anisidine (Shahidi & Wanasundara, 2002). On day 0, the values ranged from 10.38 to 14.05, whereas the values rose to 69.58 to 76.89 on day 15. Thus, the longer storage of SVDFO allowed the further lipid oxidation to take place, in which secondary oxidation products were produced. The addition of Chamomile EO with antioxidant activity (Agregán et al., 2017) into SVDFO could lower the increase in AnV of the samples when compared with the control. ICO at both concentrations could prevent the upsurge in the AnV of SVDFO during the storage. Overall, SVDFO added with CCO showed higher AnV than that incorporated with ICO, suggesting the superior preventive effect of ICO to CCO toward lipid oxidation of SVDFO.

3.3.4. Thiobarbituric acid reactive substances (TBARS)

Initially, the TBARS of all samples ranged from 0.47 to 0.52 meq MDA/ 100 g. The values of all the samples upsurged as the storage time rose, particularly during 12–15 days ($p < 0.05$) (Fig. 3b). On day 15, the TBARS value was 12.54 meq MDA/100 g for SVDFO+ICO (400) and 15.30 meq MDA/ 100 g for SVDFO or the control. Due to the autooxidation of the lipids, hydroperoxides which are generated during the primary oxidation process, were converted into aldehydes such as malondialdehyde (MDA). This MDA reacted with the thiobarbituric acid (TBA) reagent, thereby generating a pink color (Ghani et al., 2017). Greater TBARS value was associated with the higher formation of the secondary oxidation products. Lower TBARS values for the samples added with ICO and CCO might be due to the antioxidant characteristics of the EOs (Alahmady et al., 2024), including lowering the formation of hydroxyl radicals and retarding the lipid oxidation process (Caleja et al., 2015). Several antioxidative compounds, e.g. thymol, myrcene, linalool, β-zingiberene, limonene, eugenol, p-Cymene and linalool, etc. have been documented in several EOs (Alitonou et al., 2012; Gonny et al., 2004; González-Molina et al., 2010).

3.3.5. Fatty acid profiles

Fatty acid profiles of SVDFO and those containing ICO and CCO at 200 and 400 mg/L before and after storage for 15 days are presented in Table 2. All samples had oleic acid as the most abundant fatty acid (29.37–33.31 g/100 g), followed by palmitic acid (23.07–24.91 g/100 g) and linolenic acid (17.06–20.44 g /100 g). Sae-leaw and Benjakul (2017) documented that oleic acid was the most abundantly found fatty acid in the visceral lipids of Asian seabass. Tilapia (*Oreochromis* sp.) fish visceral fat had oleic acid as the most dominant fatty acid, followed by palmitic acid and palmitoleic acid (Arias et al., 2022). For PUFAs, DHA and EPA accounted for 1.50–2.55 g/100 g and 0.54–1.42 g/100 g, respectively. It has been previously reported that DHA content is generally higher than EPA in fish lipids (Song et al., 2023). BHT, which is a synthetic antioxidant, helped in stabilizing the fatty acids, in which minor variations were observed after the storage. ICO and CCO showed varying impacts on the fatty acid profile of the lipids. Generally, both EOs at higher concentrations (400 mg/L) exhibited a more pronounced

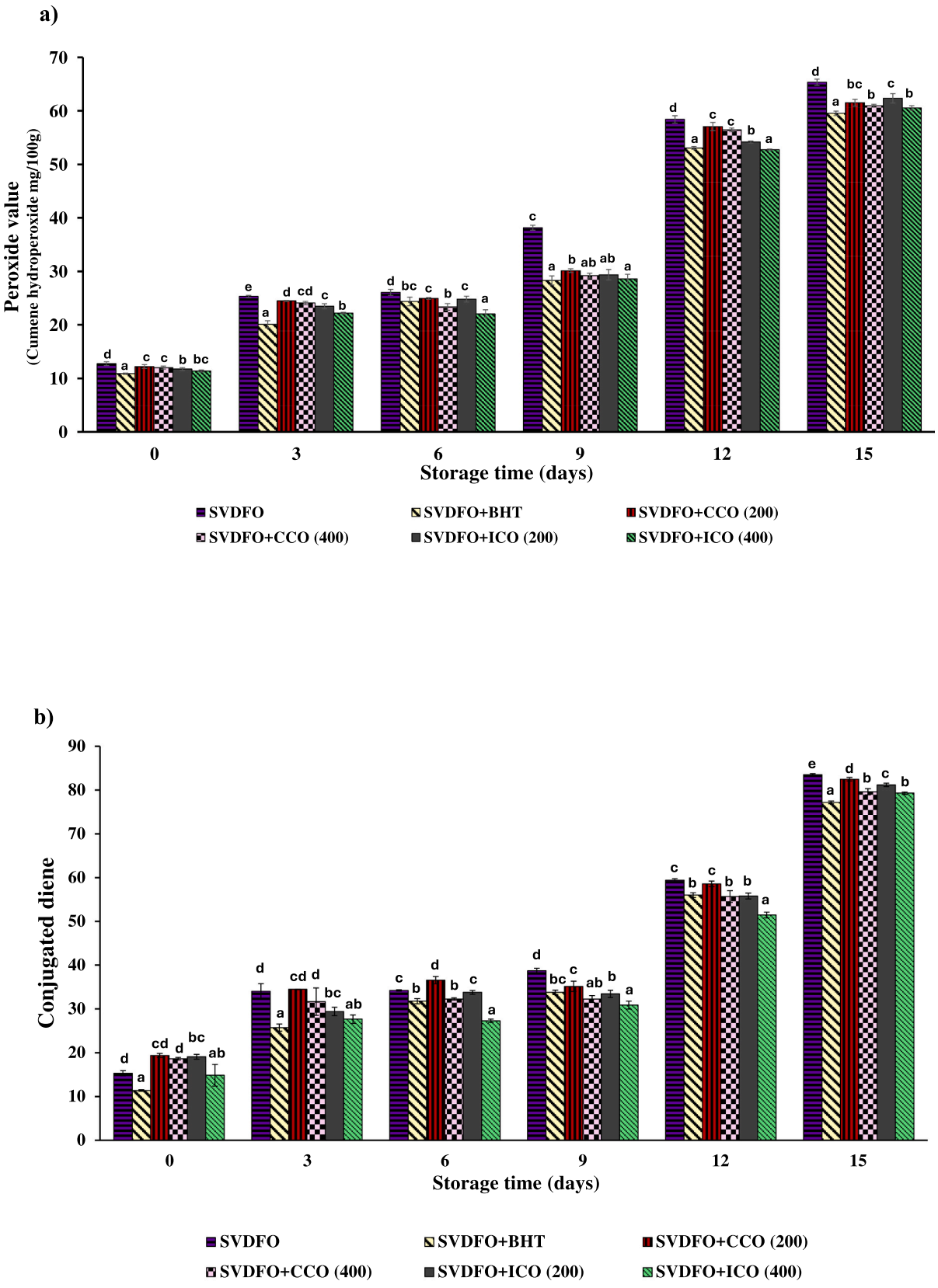

Fig. 2. Peroxide value (a) and conjugated diene (b) of Asian seabass visceral depot fat oil added with Indian and commercial Chamomile essential oils at different concentrations during the storage at room temperature. Bars represent the standard deviation ($n = 3$). Different lowercase letters within the same storage time on the bars denote the significant difference ($p < 0.05$).

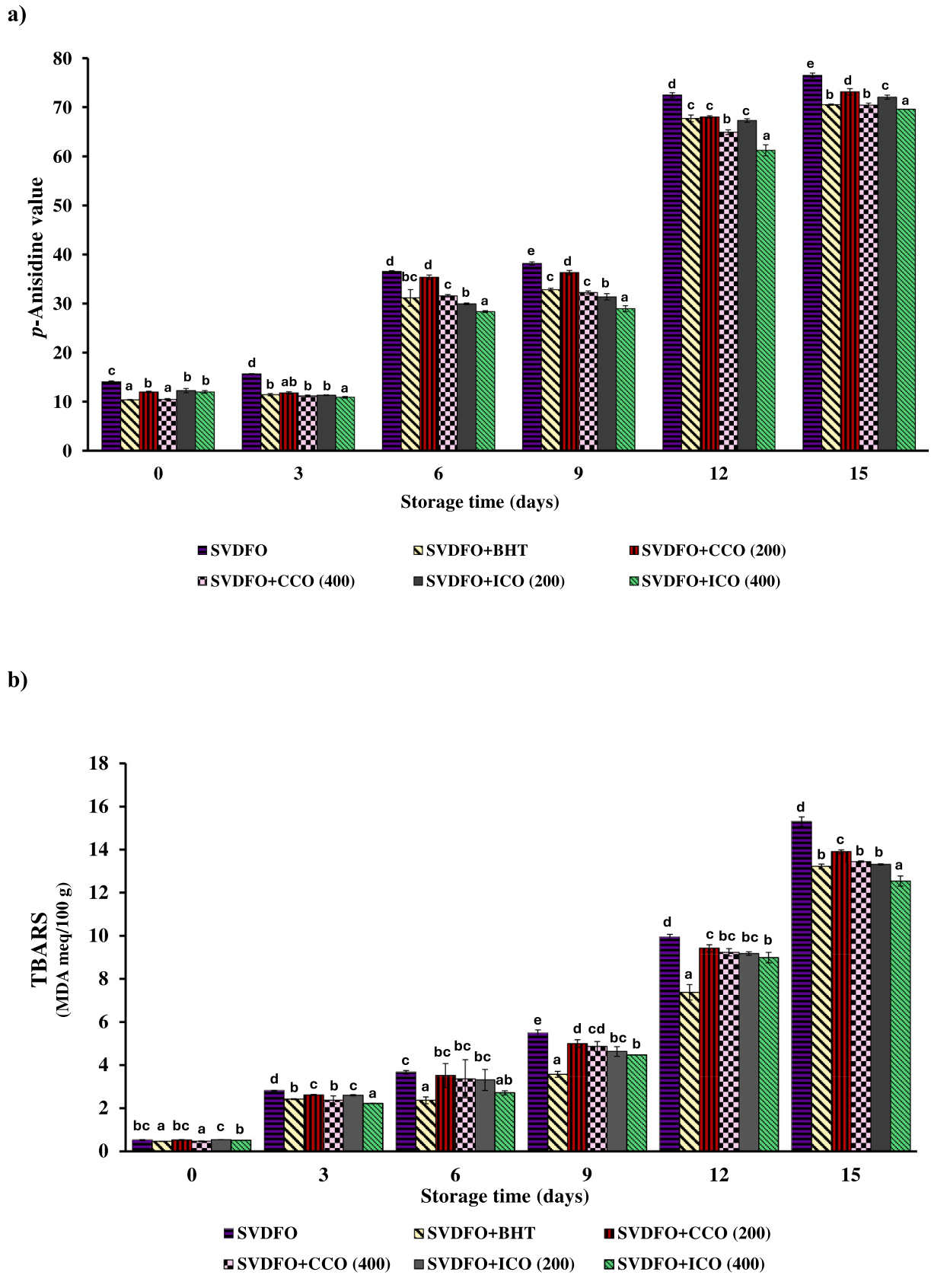

Fig. 3. *p*-Anisidine value (a) and TBARS values (b) of Asian seabass visceral depot fat oil added with Indian and commercial Chamomile essential oils at different concentrations during the storage at room temperature. Bars represent the standard deviation ($n = 3$). Different lowercase letters within the same storage time on the bars denote the significant difference ($p < 0.05$).

Table 2
Fatty acid profile of SVDFO added without and with Indian and commercial Chamomile essential oils at various concentrations before and after the storage of 15 days.

	SVDFO		SVDFO+BHT		SVDFO+CCO (200)		SVDFO+CCO (400)		SVDFO+ICO (200)		SVDFO+ICO (400)	
Fatty acids (g/100)	Day 0	Day 15	Day 0	Day 15	Day 0	Day 15	Day 0	Day 15	Day 0	Day 15	Day 0	Day 15
C6:0	0.04 ± 0.02	ND	0.02 ± 0.01	ND	0.02 ± 0.00	ND	0.02 ± 0.01	ND	0.02 ± 0.00	ND	0.05 ± 0.02	ND
C8:0	0.03 ± 0.00	ND	0.02 ± 0.00	ND	0.04 ± 0.01	ND	0.05 ± 0.00	ND	0.05 ± 0.02	ND	0.04 ± 0.02	ND
C10:0	0.03 ± 0.01	0.01 ± 0.02	0.02 ± 0.00	0.02 ± 0.02	0.02 ± 0.00	0.02 ± 0.01	0.02 ± 0.01	0.02 ± 0.01	0.02 ± 0.01	ND	0.02 ± 0.01	0.01 ± 0.00
C12:0	0.24 ± 0.00	0.18 ± 0.15	0.23 ± 0.00	0.27 ± 0.01	0.23 ± 0.01	0.26 ± 0.00	0.23 ± 0.05	0.27 ± 0.01	0.22 ± 0.00	0.26 ± 0.00	0.24 ± 0.03	0.25 ± 0.03
C14:0	2.24 ± 0.05	1.78 ± 1.00	2.19 ± 0.02	2.38 ± 0.09	2.19 ± 0.04	2.34 ± 0.02	2.01 ± 0.15	2.28 ± 0.08	2.09 ± 0.00	2.30 ± 0.01	2.13 ± 0.10	2.20 ± 0.21
C15:0	0.01 ± 0.01	ND	0.10 ± 0.15	ND	0.00 ± 0.00	ND	0.18 ± 0.15	ND	0.14 ± 0.18	ND	0.04 ± 0.04	ND
C16:0	24.23 ± 0.46	24.88 ± 0.76	23.88 ± 0.32	24.91 ± 0.81	23.94 ± 0.21	24.48 ± 0.17	23.67 ± 0.20	24.31 ± 0.25	23.91 ± 0.46	24.24 ± 0.06	23.96 ± 0.24	23.07 ± 2.25
C17:0	0.19 ± 0.04	0.21 ± 0.01	0.21 ± 0.03	0.21 ± 0.01	0.20 ± 0.01	0.19 ± 0.03	0.37 ± 0.11	0.23 ± 0.03	0.31 ± 0.07	0.20 ± 0.01	0.24 ± 0.06	0.19 ± 0.02
C18:0	6.00 ± 0.13	6.04 ± 0.19	5.95 ± 0.11	6.06 ± 0.21	5.99 ± 0.01	5.93 ± 0.02	6.21 ± 0.16	5.99 ± 0.13	6.16 ± 0.22	5.90 ± 0.03	6.12 ± 0.07	5.58 ± 0.55
C20:0	0.46 ± 0.16	0.28 ± 0.11	0.80 ± 0.63	0.36 ± 0.05	0.97 ± 0.14	0.33 ± 0.04	1.04 ± 0.07	0.56 ± 0.45	1.16 ± 0.25	0.30 ± 0.04	0.72 ± 0.69	0.33 ± 0.09
C23:0	0.03 ± 0.06	0.06 ± 0.00	0.09 ± 0.04	0.08 ± 0.02	0.11 ± 0.03	0.08 ± 0.01	0.06 ± 0.05	0.08 ± 0.00	0.09 ± 0.08	0.05 ± 0.01	0.08 ± 0.04	0.07 ± 0.01
C24:0	ND	0.09 ± 0.00	0.06 ± 0.06	0.09 ± 0.00	0.03 ± 0.06	0.06 ± 0.05	0.11 ± 0.02	0.09 ± 0.00	0.11 ± 0.01	0.09 ± 0.00	0.11 ± 0.01	0.09 ± 0.01
C14:1	0.29 ± 0.01	0.21 ± 0.11	0.19 ± 0.16	0.28 ± 0.01	0.29 ± 0.01	0.28 ± 0.01	0.21 ± 0.16	0.28 ± 0.01	0.21 ± 0.17	0.27 ± 0.01	0.31 ± 0.02	0.26 ± 0.02
C16:1	4.27 ± 0.06	2.91 ± 2.52	4.09 ± 0.03	2.88 ± 2.49	4.10 ± 0.08	4.33 ± 0.03	3.79 ± 0.25	4.23 ± 0.14	3.90 ± 0.06	4.27 ± 0.01	3.94 ± 0.19	9.69 ± 9.34
C17:1	0.07 ± 0.01	0.08 ± 0.01	0.08 ± 0.00	0.08 ± 0.00	0.07 ± 0.00	0.07 ± 0.00	0.07 ± 0.01	0.07 ± 0.00	0.08 ± 0.01	0.07 ± 0.00	0.07 ± 0.01	0.07 ± 0.01
C18:1 n-7	0.17 ± 0.06	0.10 ± 0.09	0.13 ± 0.11	0.18 ± 0.02	0.08 ± 0.09	0.10 ± 0.10	0.10 ± 0.09	0.10 ± 0.08	0.12 ± 0.06	0.00 ± 0.00	0.06 ± 0.06	0.09 ± 0.08
C18:1 n-9	32.99 ± 0.34	33.31 ± 0.98	31.62 ± 0.45	33.08 ± 0.93	31.70 ± 0.82	32.59 ± 0.33	29.37 ± 2.02	32.22 ± 0.65	29.96 ± 0.69	32.35 ± 0.07	30.22 ± 1.07	30.84 ± 3.08
C20:1	0.52 ± 0.46	1.88 ± 0.08	1.72 ± 0.13	1.75 ± 0.12	1.40 ± 0.50	1.69 ± 0.12	1.45 ± 0.07	1.74 ± 0.18	1.23 ± 0.40	1.82 ± 0.09	1.02 ± 0.48	1.69 ± 0.32
C22:1	ND	0.09 ± 0.03	0.05 ± 0.04	0.08 ± 0.00	0.05 ± 0.04	0.08 ± 0.00	0.06 ± 0.00	0.07 ± 0.01	0.06 ± 0.01	0.07 ± 0.01	0.05 ± 0.04	0.07 ± 0.01
C24:1	ND	0.10 ± 0.01	ND	0.09 ± 0.00	ND	0.09 ± 0.01	ND	0.10 ± 0.02	ND	0.09 ± 0.01	ND	0.09 ± 0.02
C18:2 n-6	20.20 ± 0.30	17.31 ± 1.36	19.17 ± 0.33	20.35 ± 0.67	19.32 ± 0.51	19.76 ± 0.23	17.06 ± 1.68	19.42 ± 0.52	17.66 ± 0.74	19.81 ± 0.03	18.01 ± 1.18	20.33 ± 2.13
C18:2	0.22 ± 0.39	0.45 ± 0.39	0.64 ± 0.02	0.68 ± 0.03	0.21 ± 0.36	0.66 ± 0.01	0.57 ± 0.05	0.64 ± 0.02	0.59 ± 0.02	0.65 ± 0.01	0.42 ± 0.36	0.76 ± 0.14
C18:3	0.10 ± 0.02	1.01 ± 0.03	0.70 ± 0.50	0.39 ± 0.52	0.60 ± 0.43	0.68 ± 0.52	0.75 ± 0.15	0.95 ± 0.04	0.81 ± 0.07	0.98 ± 0.00	0.33 ± 0.41	0.35 ± 0.05
C20:2	0.30 ± 0.26	0.46 ± 0.04	0.44 ± 0.01	0.44 ± 0.02	0.45 ± 0.01	0.44 ± 0.03	0.41 ± 0.02	0.44 ± 0.02	0.44 ± 0.03	0.44 ± 0.01	0.45 ± 0.01	0.45 ± 0.06
C20:3	0.14 ± 0.03	0.16 ± 0.00	0.14 ± 0.02	0.16 ± 0.00	0.17 ± 0.00	0.17 ± 0.00	0.13 ± 0.01	0.15 ± 0.02	0.13 ± 0.01	0.15 ± 0.02	0.15 ± 0.02	0.21 ± 0.02
C20:4	0.65 ± 0.01	0.66 ± 0.02	0.68 ± 0.07	0.66 ± 0.02	0.71 ± 0.06	0.63 ± 0.01	1.33 ± 0.51	0.71 ± 0.13	1.07 ± 0.14	0.64 ± 0.00	1.01 ± 0.29	1.11 ± 0.12
C20:5	1.08 ± 0.01	0.54 ± 0.04	1.22 ± 0.57	1.10 ± 0.06	1.08 ± 0.03	1.06 ± 0.04	1.42 ± 0.30	1.39 ± 0.06	1.29 ± 0.06	1.28 ± 0.02	1.27 ± 0.16	1.22 ± 0.14
C22:2	0.37 ± 0.32	0.36 ± 0.09	0.15 ± 0.26	0.26 ± 0.23	0.37 ± 0.33	0.00 ± 0.00	0.24 ± 0.22	0.11 ± 0.20	0.37 ± 0.32	0.22 ± 0.19	0.50 ± 0.13	0.48 ± 0.03
C22:6	2.03 ± 0.52	1.50 ± 0.48	2.55 ± 0.51	2.41 ± 0.50	2.42 ± 0.77	2.36 ± 0.05	2.52 ± 1.61	2.48 ± 1.05	2.42 ± 1.46	2.40 ± 0.01	2.50 ± 1.65	2.44 ± 0.20
SFAs	33.65 ± 1.07^{a}	36.76 ± 1.45^{b}	33.81 ± 1.38^{ab}	34.60 ± 1.11^{ab}	33.98 ± 0.53^{ab}	34.30 ± 0.23^{ab}	34.19 ± 0.99^{ab}	34.05 ± 0.45^{ab}	34.52 ± 1.32^{ab}	33.56 ± 0.06^{a}	33.99 ± 1.34^{ab}	33.82 ± 1.13^{a}
MUFAs	38.31 ± 0.94^{ab}	38.70 ± 1.96^{ab}	37.86 ± 0.93^{ab}	38.42 ± 1.57^{ab}	37.70 ± 1.54^{ab}	39.22 ± 0.39^{ab}	35.09 ± 2.69^{a}	38.81 ± 0.88^{ab}	35.63 ± 1.46^{a}	38.93 ± 0.08^{ab}	35.78 ± 1.86^{a}	35.92 ± 0.55^{b}
PUFAs	25.13 ± 1.88^{b}	21.85 ± 0.87^{a}	25.41 ± 2.36^{b}	25.99 ± 0.50^{b}	25.41 ± 2.58^{b}	25.89 ± 0.61^{b}	27.80 ± 6.60^{b}	26.15 ± 0.67^{b}	26.94 ± 2.90^{b}	26.52 ± 0.13^{b}	27.32 ± 5.15^{b}	27.37 ± 0.60^{b}

ND - not detected; SFA – Saturated Fatty Acids; MUFA – Mono-unsaturated Fatty Acids; PUFA – Poly Unsaturated Fatty Acids, Values are Mean ± SD ($n = 3$). Different lowercase superscripts in the same row denote significant differences ($p < 0.05$).

impact on the stabilization of SVDFO, especially PUFAs such as DHA and EPA. The fatty acid profile clearly suggested that the EOs influenced the SVDFO by maintaining the levels of DHA and EPA. The control sample showed the decrease in DHA by 2.03–1.50 g/100 g after the 15th day of storage, whereas the SVDFO incorporated with EO had the less decrease, in comparison with the control. Furthermore, the EPA levels of the control sample was 1.08 g/100 g which was lowered to 0.54 g/100 g after 15 days. EPA of other samples seemed to be maintained after the storage. In the present study, PUFAs of the control decreased ($p < 0.05$) after the storage. Nonetheless, the samples containing antioxidants were less oxidized as indicated by the negligible decrease ($p > 0.05$). During the storage, SFAs tended to be more stable during storage with minor changes [65]. For the control, the slight increase in SFAs was observed ($p < 0.05$). This was more likely due to the higher proportion of SFAs retained in SVDFO. No differences in SFAs among other samples were found ($p > 0.05$). MUFA showed high variations among the samples with respect to type and concentrations of EOs. PUFAs present in fish lipids are more sensitive to storage conditions and oxidation could be retarded by incorporation with EOs, especially ICO at higher concentration. EOs have been known to contain several antioxidative compounds (Hassoun & Emir Çoban, 2017).

3.3.6. FTIR spectra

FTIR spectra of SVDFO and EO added samples stored at 30 °C on the final 15th day are illustrated in Fig. 4. Primary functional groups which are responsible for FTIR absorption peaks were as follows: the C—H stretching vibration of the cis-double bond at 3015 cm^{-1}, asymmetric at 2850 cm^{-1} and symmetric at 2920 cm^{-1} stretching vibrations of CH_2, C═O stretching vibration of the ester group in the triacylglycerols at 1740 cm^{-1}, CH_2 scissor vibration at 1460 cm^{-1}, CH_2 bending vibration at 1375 cm^{-1}, out-of-plane deformation at 1150 cm^{-1} and the CH_2 rocking vibration at 720 cm^{-1} (Pudtikajorn et al., 2022; Sae-leaw & Benjakul, 2017). During the storage period, the double bonds inside the SVDFO samples (without antioxidant) underwent oxidation and were reduced as figured out by the reduction of the peak amplitude at 3015 cm^{-1} (Fig. 4). EOs added into SVDFO samples could prevent the reduction of the 3015 cm^{-1} peak. The result revealed that Chamomile EOs could retard the lipid oxidation process. Moreover, due to the prolonged exposure to temperature and oxygen, the ester bonds present in the triacylglycerols were cleaved during the storage period (Machado et al., 2023). The decrease in the strength of the wavenumber 1745 cm^{-1} suggested that a decrease in the intensity of the ester bonds took place at a longer storage time (Fig. 4). Similarly, the EO treated samples showed a positive trend in preventing the decomposition or breakdown of the ester bonds present in the SVDFO samples (Kunyaboon et al., 2021; Sae-leaw & Benjakul, 2014).

In addition, the peak at 3600–3400 cm^{-1} representing hydroperoxide was higher in amplitude in the SVDFO (control) than those added

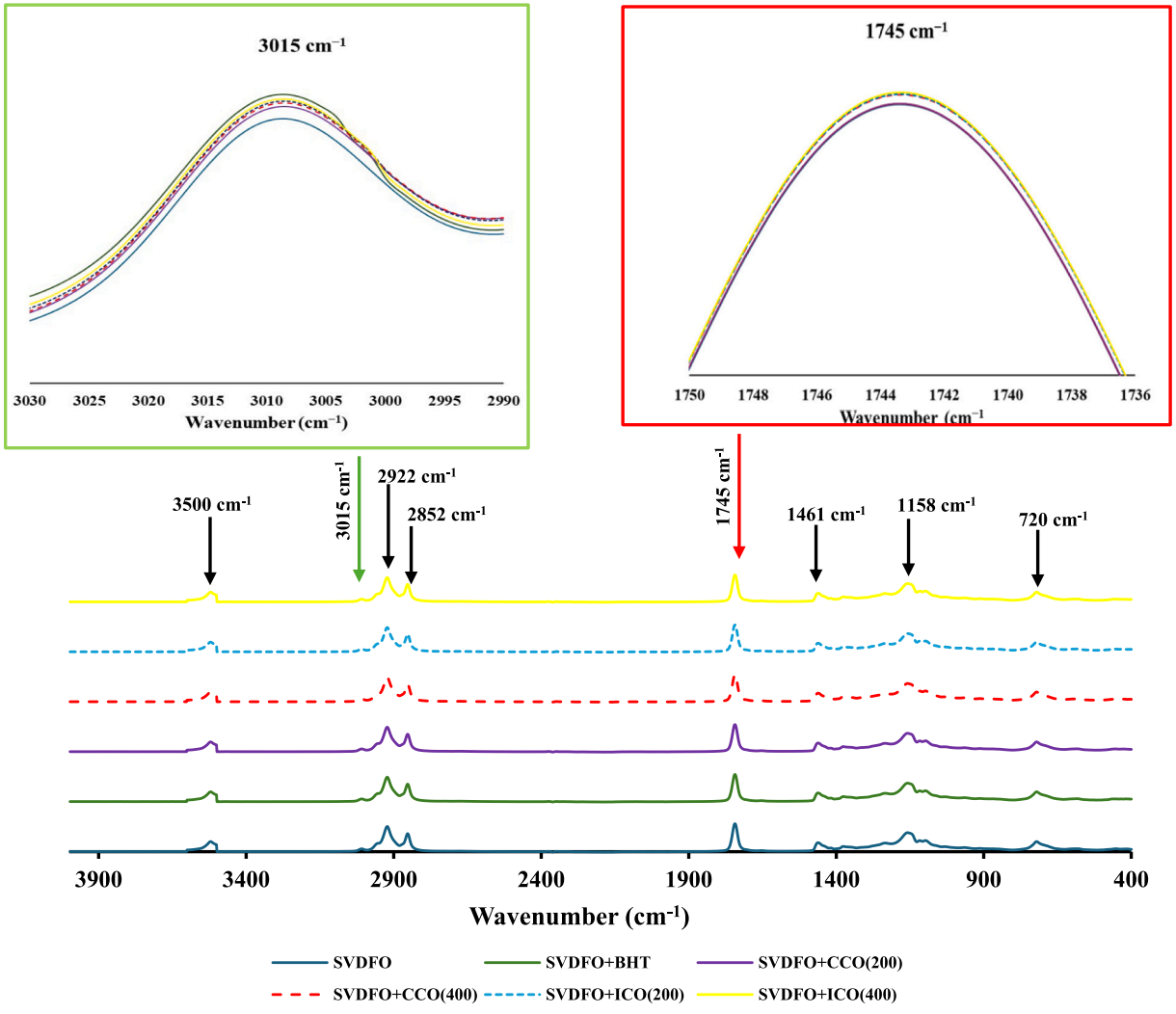

Fig. 4. FTIR spectra of SVDFO lipid samples without and with addition of Indian and commercial Chamomile essential oils at different concentrations at final 15th day at room temperature with special emphasis on FTIR spectra at 1745 cm^{-1} and 3010 cm^{-1}.

with either ICO or CCO. However, the lower peak amplitude was observed in the sample containing ICO than that added with CCO. This confirmed the higher preventive effect of ICO against oxidation than CCO. This result was in tandem with higher PV, TBARS and AnV in the latter.

3.3.7. Color values

L^*, a^*, b^* color values of all oil samples before and after storage for 15 days are presented in Table 3. All the samples showed an increase in the L^* values, indicating the lighter color of SVDFO after 15 days. The increase in lightness was comparatively consistent across all the samples, in which SVDFO showed the highest increase in L^* values from 99.85 to 100.44. The a^* values of all the samples showed a decreasing trend, which was related to the shift to greenish color. The decrease was more pronounced in the samples with higher concentrations (400 mg/L) of both ICO and CCO, which might be due to the unique greenish-blue color of the Chamomile EOs. There was a decrease in the b^* values for SVDFO from 3.65 to 3.39, which indicated that the color had a slight shift toward blue. For SVDFO+BHT, the b^* remained almost unchanged. BHT more likely helped in keeping the yellow color of SVDFO, which was yellowish in color. The samples added with ICO and CCO showed a non-significant change in the b^* values. These results were in accordance with a previous study, where EOs from cinnamon and rosemary showed good color stability in the meat samples (Semenova et al., 2019).

Table 3
L^*, a^* and b^* values of SVDFO added without and with Indian and commercial Chamomile essential oils at various concentrations before and after the storage of 15 days.

	L^*		a^*		b^*	
	Day 0	Day 15	Day 0	Day 15	Day 0	Day 15
SVDFO	99.85 ± 0.03^{c}	100.44 ± 0.01^{e}	−1.28 ± 0.00^{i}	−1.55 ± 0.01^{d}	3.65 ± 0.00^{b}	3.39 ± 0.01^{a}
SVDFO+BHT	99.70 ± 0.01^{b}	100.40 ± 0.01^{e}	−1.28 ± 0.01^{i}	−1.54 ± 0.00^{e}	3.64 ± 0.00^{b}	3.64 ± 0.01^{b}
SVDFO+CCO (200)	99.82 ± 0.01^{c}	100.41 ± 0.00^{e}	−1.36 ± 0.00^{g}	−1.62 ± 0.00^{b}	3.81 ± 0.01^{cd}	3.87 ± 0.00^{d}
SVDFO+CCO (400)	98.98 ± 0.14^{a}	100.31 ± 0.01^{d}	−1.32 ± 0.02^{h}	−1.68 ± 0.01^{a}	3.77 ± 0.04^{c}	3.94 ± 0.16^{d}
SVDFO+ICO (200)	99.84 ± 0.01^{c}	100.38 ± 0.00^{d}	−1.33 ± 0.00^{h}	−1.61 ± 0.00^{c}	3.68 ± 0.00^{bc}	3.83 ± 0.01^{cd}
SVDFO+ICO (400)	99.68 ± 0.03^{b}	100.32 ± 0.00^{d}	−1.41 ± 0.01^{f}	−1.67 ± 0.00^{a}	3.71 ± 0.01^{bc}	3.69 ± 0.22^{bc}

Values are Mean ± SD (n = 3). Different lowercase superscripts in the same column denote significant differences ($p < 0.05$).

4. Conclusion

Chamomile essential oils possessed significant antioxidant activity, attributed to the presence of bioactive components. Both ICO and CCO exhibited strong antioxidant properties and effectively inhibited the oxidation of SVDFO. The ability to retard lipid oxidation was enhanced with increasing concentrations of ICO and CCO, indicating a dose-dependent effect. Among the tested samples, ICO at 400 mg/L showed the highest efficacy in preventing lipid oxidation in SVDFO, compared to CCO at the same concentration during the initial 12 days of storage. Furthermore, the incorporation of chamomile EOs helped preserve the monounsaturated fatty acid (MUFA) and polyunsaturated fatty acid (PUFA) contents of the oil throughout the storage period, highlighting their protective role against lipid oxidation. Therefore, chamomile EO had the potential to serve as a natural antioxidant for stabilizing PUFA-rich oils, offering an alternative to synthetic antioxidants. Additionally, the antioxidant effectiveness of chamomile EO was found to be influenced by its geographic origin, emphasizing the importance of sourcing and environmental factors in determining its bioactivity. Future studies will further explore bioactivities and the applications of EOs for food preservation.

Funding

The research work was supported by the Prince of Songkla University (PSU), Hat Yai under the National Research Council of Thailand (NRCT) Research Chair Grant (N42A670596).

CRediT authorship contribution statement

Birinchi Bora: Writing – original draft, Software, Methodology, Investigation, Formal analysis, Data curation, Conceptualization. **Tao Yin:** Writing – review & editing, Data curation. **Bin Zhang:** Writing – review & editing, Data curation. **Can Okan Altan:** Writing – review & editing, Data curation. **Soottawat Benjakul:** Writing – review & editing, Validation, Supervision, Resources, Project administration, Conceptualization.

Declaration of competing interest

The authors declare that they have no known competing financial interests or personal relationships that could have appeared to influence the work reported in this paper.

Data availability

Data will be made available on request.

References

Ababouch, L., & Vannuccini, S. (2024). FAO the state of world fisheries and aquaculture 2024—Blue transformation in action. In *In: FAO Geneva*. Switzerland: Retrived from. http://openknowledge.fao.org/items/06690fd0-d133-424c-9673-1849e414543d Accessed August 21, 2024.

Abeyrathne, E. D. N. S., Nam, K., & Ahn, D. U. (2021). Analytical methods for lipid oxidation and antioxidant capacity in food systems. *Antioxidants, 10*(10), 1587. https://www.mdpi.com/2076-3921/10/10/1587.

Agregán, R., Lorenzo, J. M., Munekata, P. E. S., Dominguez, R., Carballo, J., & Franco, D. (2017). Assessment of the antioxidant activity of *Bifurcaria bifurcata* aqueous extract on canola oil. Effect of extract concentration on the oxidation stability and volatile compound generation during oil storage. *Food Research International, 99*, 1095–1102. https://doi.org/10.1016/j.foodres.2016.10.029

Ahmad, A. S., Sae-Leaw, T., Zhang, B., & Benjakul, S. (2024). Antioxidant and antimicrobial activities of ethanolic jik (*Barringtonia acutangula*) leaf extract and its application for shelf-life extension of Pacific white shrimp meat during refrigerated storage. *Food Control, 155*, Article 110037. https://doi.org/10.1016/j.foodcont.2023.110037

Ahmmed, M. K., Ahmmed, F., Tian, H., Carne, A., & Bekhit, A. E. D. (2020). Marine omega-3 (n-3) phospholipids: A comprehensive review of their properties, sources, bioavailability, and relation to brain health. *Comprehensive Reviews in Food Science and Food Safety, 19*(1), 64–123. https://doi.org/10.1111/1541-4337.12510

Alahmady, N. F., Alkhulaifi, F. M., Abdullah Momenah, M., Ali Alharbi, A., Allohibi, A., Alsubhi, N. H., & Ahmed Alhazmi, W. (2024). Biochemical characterization of chamomile essential oil: Antioxidant, antibacterial, anticancer and neuroprotective activity and potential treatment for Alzheimer's disease. *Saudi Journal of Biological Sciences, 31*(2), Article 103912. https://doi.org/10.1016/j.sjbs.2023.103912

Al-Dabbagh, B., Elhaty, I. A., Elhaw, M., Murali, C., Al Mansoori, A., Awad, B., & Amin, A. (2019). Antioxidant and anticancer activities of chamomile (*Matricaria recutita* L.). *BMC Research Notes, 12*(1), 3. https://doi.org/10.1186/s13104-018-3960-y

Alfio, V. G., Manzo, C., & Micillo, R. (2021). From fish waste to value: An overview of the sustainable recovery of omega-3 for food supplements. *Molecules, 26*(4), 1002. https://doi.org/10.3390/molecules26041002

Alitonou, G. A., Tchobo, F. P., Avlessi, F., Yehouenou, B., Yedomonhan, P., Koudoro, A. Y., & Sohounhloue, D. K. (2012). Chemical and biological investigations of *Syzygium aromaticum* L. essential oil from Benin. *International Journal of Biological and Chemical Sciences, 6*(3), 1360–1367. https://doi.org/10.4314/ijbcs.v6i3.37

Amigo-Benavent, M., Khalesi, M., Thapa, G., & FitzGerald, R. J. (2021). Chapter 6 - methodologies for bioactivity assay: Biochemical study. In F. Toldrá, & J. Wu (Eds.), *Biologically active peptides* (pp. 103–153). Academic Press.

Amiri, H. (2012). Essential oils composition and antioxidant properties of three Thymus species. *Evidence-based Complementary and Alternative Medicine, 2012*(1), Article 728065. https://doi.org/10.1155/2012/728065

Anandakumar, P., Kamaraj, S., & Vanitha, M. K. (2021). D-limonene: A multifunctional compound with potent therapeutic effects. *Journal of Food Biochemistry, 45*(1), Article e13566. https://doi.org/10.1111/jfbc.13566

Arias, L., Marquez, D. M., & Zapata, J. E. (2022). Quality of red tilapia viscera oil (*Oreochromis sp.*) as a function of extraction methods. *Heliyon, 8*(5). https://doi.org/10.1016/j.heliyon.2022.e09546

Barreto, R. S. S., Quintans, J. S. S., Amarante, R. K. L., Nascimento, T. S., Amarante, R. S., Barreto, A. S., & Quintans-Júnior, L. J. (2016). Evidence for the involvement of TNF-α and IL-1β in the antinociceptive and anti-inflammatory activity of *Stachys lavandulifolia* Vahl. (*Lamiaceae*) essential oil and (−)-α-bisabolol, its main compound, in mice. *Journal of Ethnopharmacology, 191*, 9–18. https://doi.org/10.1016/j.jep.2016.06.022

Benjakul, S., Sae-leaw, T., & Simpson, B. K. (2019). Byproducts from fish harvesting and processing. In *, 179-217. Byproducts from agriculture and fisheries: adding value for food, feed, pharma, and fuels*. https://doi.org/10.1002/9781119383956.ch9

Bozova, B., Gölükcü, M., & Giuffrè, A. M. (2024). The effect of different hydrodistillation times on the composition and yield of bergamot (*Citrus bergamia Risso*) peel essential oil and a comparison of the cold-pressing method. *Flavour and Fragrance Journal, 39*(5), 263–270. https://doi.org/10.1002/ffj.3789

Caleja, C., Barros, L., Antonio, A. L., Ciric, A., Barreira, J. C. M., Sokovic, M., & Ferreira, I. C. F. R. (2015). Development of a functional dairy food: Exploring bioactive and preservation effects of chamomile (*Matricaria recutita* L.). *Journal of Functional Foods, 16*, 114–124. https://doi.org/10.1016/j.jff.2015.04.033

Candido, G. S., Natarelli, C. V. L., Carvalho, E. E. N., & Oliveira, J. E. (2022). Bionanocomposites of pectin and pracaxi oil nanoemulsion as active packaging for butter. *Food Packaging and Shelf Life, 32*, Article 100862. https://doi.org/10.1016/j.fpsl.2022.100862

Capuzzo, A., Occhipinti, A., & Maffei, M. E. (2014). Antioxidant and radical scavenging activities of chamazulene. *Natural Product Research, 28*(24), 2321–2323. https://doi.org/10.1080/14786419.2014.931393

Chauhan, R., Singh, S., Kumar, V., Kumar, A., Kumari, A., Rathore, S., & Singh, S. (2022). A comprehensive review on biology, genetic improvement, agro and process Technology of German Chamomile (*Matricaria chamomilla* L.). *Plants, 11*(1), 29. https://doi.org/10.3390/plants11010029

Dale, H. F., Madsen, L., & Lied, G. A. (2019). Fish–derived proteins and their potential to improve human health. *Nutrition Reviews, 77*(8), 572–583. https://doi.org/10.1093/nutrit/nuz016

El Mihyaoui, A., Esteves da Silva, J. C. G., Charfi, S., Candela Castillo, M. E., Lamarti, A., & Arnao, M. B. (2022). Chamomile (*Matricaria chamomilla* L.): A review of Ethnomedicinal use, Phytochemistry and pharmacological uses. *Life, 12*(4), 479. https://doi.org/10.3390/life12040479

Gabbanini, S., Neba, J. N., Matera, R., & Valgimigli, L. (2024). Photochemical and oxidative degradation of Chamazulene contained in Artemisia, Matricaria and Achillea essential oils and setup of protection strategies. *Molecules, 29*(11), 2604. https://doi.org/10.3390/molecules29112604

Ghani, M. A., Barril, C., Bedgood, D. R., & Prenzler, P. D. (2017). Measurement of antioxidant activity with the thiobarbituric acid reactive substances assay. *Food Chemistry, 230*, 195–207. https://doi.org/10.1016/j.foodchem.2017.02.127

Gölükcü, M., Bozova, B., Tokgöz, H., Turgut, D. Y., Çınar, O., Turgutoglu, E., & Giuffrè, A. M. (2024). Effects of cultivar, harvesting time and isolation techniques on the essential oil compositions of some lemon cultivars. *AIMS Agriculture and Food, 9*(3). https://doi.org/10.3934/agrfood.2024049

Gonny, M., Bradesi, P., & Casanova, J. (2004). Identification of the components of the essential oil from wild *Corsican Daucus carota* L. using 13C-NMR spectroscopy. *Flavour and Fragrance Journal, 19*(5), 424–433. https://doi.org/10.1002/ffj.1330

González-Molina, E., Domínguez-Perles, R., Moreno, D. A., & García-Viguera, C. (2010). Natural bioactive compounds of Citrus Limon for food and health. *Journal of Pharmaceutical and Biomedical Analysis, 51*(2), 327–345. https://doi.org/10.1016/j.jpba.2009.07.027

Hassoun, A., & Emir Çoban, Ö. (2017). Essential oils for antimicrobial and antioxidant applications in fish and other seafood products. *Trends in Food Science and Technology, 68*, 26–36. https://doi.org/10.1016/j.tifs.2017.07.016

Huang, X., & Ahn, D. U. (2019). Lipid oxidation and its implications to meat quality and human health. *Food Science and Biotechnology, 28*(5), 1275–1285. https://doi.org/10.1007/s10068-019-00631-7

IFFO. (2022). The Marine Ingredients Organization. In *Annual report*. Retrived from https://www.iffo.com/annual-report-2022 Accessed July 28, 2024.

Jacobsen, C., García-Moreno, P. J., Yesiltas, B., & Sørensen, A.-D. M. (2021). Chapter 9 - lipid oxidation and traditional methods for evaluation. In P. J. García-Moreno, C. Jacobsen, A.-D. Moltke Sørensen, & B. Yesiltas (Eds.), *Omega-3 Delivery Systems* (pp. 183–200). Academic Press.

Khan, M. S. A., & Ahmad, I. (2019). Herbal medicine: Current trends and future prospects. In *New look to phytomedicine* (pp. 3–13). Elsevier.

Kunyaboon, S., Thumanu, K., Park, J. W., Khongla, C., & Yongsawatdigul, J. (2021). Evaluation of lipid oxidation, volatile compounds and vibrational spectroscopy of silver carp (*Hypophthalmichthys molitrix*) during ice storage as related to the quality of its washed mince. *Foods, 10*(3), 495. https://doi.org/10.3390/foods10030495

Lauritzen, L. (2021). Seafood assessed for global human nutrition. *Nature: International Weekly Journal of Science*, 7880.

Lertchirakarn, P., & Muangrat, R. (2023). Antibacterial efficacy of essential oils from four spices against *salmonella typhimurium*: Mathematical modelling and application in enhancing salad cream safety. *Current Research in Nutrition and Food Science Journal, 11*(3), 1282–1299. https://doi.org/10.12944/CRNFSJ.11.3.30

Li, Q., Sun, X., Mubango, E., Zheng, Y., Liu, Y., Zhang, Y., & Hong, H. (2023). Effects of protein and lipid oxidation on the water holding capacity of different parts of bighead carp: Eye, dorsal, belly and tail muscles. *Food Chemistry, 423*, Article 136238. https://doi.org/10.1016/j.foodchem.2023.136238

Li, Y., Ma, H., Wan, Y., Li, T., Liu, X., Sun, Z., & Li, Z. (2016). Volatile organic compounds emissions from *Luculia pinceana* flower and its changes at different stages of flower development. *Molecules, 21*(4), 531. https://doi.org/10.3390/molecules21040531

Lim, H. S., Kim, S. K., Woo, S.-G., Kim, T. H., Yeom, S.-J., Yong, W., & Lee, D.-H. (2021). (−)-α-Bisabolol production in engineered *Escherichia coli* expressing a novel (−)-α-Bisabolol synthase from the globe artichoke *Cynara cardunculus* var. *Scolymus*. *Journal of Agricultural and Food Chemistry, 69*(30), 8492–8503. https://doi.org/10.1021/acs.jafc.1c02759

Machado, M., Rodriguez-Alcalá, L. M., Gomes, A. M., & Pintado, M. (2023). Vegetable oils oxidation: Mechanisms, consequences and protective strategies. *Food Reviews International, 39*(7), 4180–4197. https://doi.org/10.1080/87559129.2022.2026378

Meeran, M. F. N., Laham, F., Al-Taee, H., Azimullah, S., & Ojha, S. (2018). Protective effects of α-bisabolol on altered hemodynamics, lipid peroxidation, and nonenzymatic antioxidants in isoproterenol-induced myocardial infarction: *In vivo* and *in vitro* evidences. *Journal of Biochemical and Molecular Toxicology, 32*(10), Article e22200. https://doi.org/10.1002/jbt.22200

Mittal, A., Singh, A., Hong, H., & Benjakul, S. (2023). Chitooligosaccharides from shrimp shell chitosan prepared using H_2O_2 or ascorbic acid/H_2O_2 redox pair hydrolysis: Characteristics, antioxidant and antimicrobial activities. *International Journal of Food Science and Technology, 58*(5), 2645–2660. https://doi.org/10.1111/ijfs.15696

Miyashita, K., Uemura, M., & Hosokawa, M. (2018). Effective prevention of oxidative deterioration of fish oil: Focus on flavor deterioration. *Annual Review of Food Science and Technology, 9*(1), 209–226. https://doi.org/10.1146/annurev-food-030117-012320

Miyazawa, T. (2021). Lipid hydroperoxides in nutrition, health, and diseases. *Proceedings of the Japan Academy, Series B, 97*(4), 161–196. https://doi.org/10.2183/pjab.97.010

Nazlić, M., Kremer, D., Grubešić, R. J., Soldo, B., Vuko, E., Stabentheiner, E., & Dunkić, V. (2020). Endemic *Veronica saturejoides Vis*. Ssp. *saturejoides*–chemical composition and antioxidant activity of free volatile compounds. *Plants, 9*(12), 1646. https://doi.org/10.3390/plants9121646

Pathania, V., Bora, B., Kumar, R., Sharma, K., Neha, Y., Kumar, A., & Srivatsan, V. (2024). Valorization of German chamomile Agri-waste as a source of high-value products: Characterization of nutrients and phytochemicals towards functional food development. *Waste and Biomass Valorization*. https://doi.org/10.1007/s12649-024-02683-1

Patil, U., & Benjakul, S. (2019). Physical and textural properties of mayonnaise prepared using virgin coconut oil/fish oil blend. *Food Biophysics, 14*, 260–268. https://doi.org/10.1007/s11483-019-09579-x

Piri, E., Mahmoodi Sourestani, M., Khaleghi, E., Mottaghipisheh, J., Zomborszki, Z. P., Hohmann, J., & Csupor, D. (2019). Chemo-diversity and antiradical potential of twelve *Matricaria chamomilla* L. populations from Iran: Proof of ecological effects. *Molecules, 24*(7), 1315. https://doi.org/10.3390/molecules24071315

Pudtikajorn, K., & Benjakul, S. (2020). Simple wet rendering method for extraction of prime quality oil from skipjack tuna eyeballs. *European Journal of Lipid Science and Technology, 122*(8), 2000077. https://doi.org/10.1002/ejlt.202000077

Pudtikajorn, K., Sae-leaw, T., Singh, A., & Benjakul, S. (2022). Mild heating process and antioxidant incorporation increase quality and oxidation stability of oil from skipjack tuna (*Katsuwonus pelamis*) eyeball. *European Journal of Lipid Science and Technology, 124*(3), 2000391. https://doi.org/10.1002/ejlt.202000391

Rajasekaran, B., Gulzar, S., Gopalrajan, S., Karunanithi, M., & Benjakul, S. (2024). Omega-3 enriched fish and shellfish oils: Extraction, preservation, and health benefits. In *Fish waste to valuable products* (pp. 195–229). Springer.

Raju, N., Gulzar, S., Buamard, N., Ma, L., Ying, X., Zhang, B., & Benjakul, S. (2021). Comparative study of Astaxanthin, cholesterol, fatty acid profiles, and quality indices between shrimp oil extracted from Hepatopancreas and cephalothorax. *Frontiers in Nutrition, 8*. https://doi.org/10.3389/fnut.2021.803664

Ramazani, E., Akaberi, M., Emami, S. A., & Tayarani-Najaran, Z. (2022). Pharmacological and biological effects of alpha-bisabolol: An updated review of the molecular mechanisms. *Life Sciences, 304*, Article 120728. https://doi.org/10.1016/j.lfs.2022.120728

Rathore, S., & Kumar, R. (2021). Agronomic interventions affect the growth, yield, and essential oil composition of German chamomile (*Matricaria chamomilla* L.) in the western Himalaya. *Industrial Crops and Products, 171*, Article 113873. https://doi.org/10.1016/j.indcrop.2021.113873

Sae-leaw, T., & Benjakul, S. (2014). Fatty acid composition, lipid oxidation, and fishy odour development in seabass (*Lates calcarifer*) skin during iced storage. *European Journal of Lipid Science and Technology, 116*(7), 885–894. https://doi.org/10.1002/ejlt.201300381

Sae-leaw, T., & Benjakul, S. (2017). Lipids from visceral depot fat of Asian seabass (*Lates calcarifer*): Compositions and storage stability as affected by extraction methods. *European Journal of Lipid Science and Technology, 119*(11), 1700198. https://doi.org/10.1002/ejlt.201700198

Sae-leaw, T., O'Callaghan, Y. C., Benjakul, S., & O'Brien, N. M. (2016). Antioxidant activities and selected characteristics of gelatin hydrolysates from seabass (*Lates calcarifer*) skin as affected by production processes. *Journal of Food Science and Technology, 53*(1), 197–208. https://doi.org/10.1007/s13197-015-1989-7

Saha, A., & Basak, B. (2020). Scope of value addition and utilization of residual biomass from medicinal and aromatic plants. *Industrial Crops and Products, 145*, Article 111979. https://doi.org/10.1016/j.indcrop.2019.111979

Saleh, N. E., Wassef, E. A., & Abdel-Mohsen, H. H. (2022). Sustainable fish and seafood production and processing. In *Sustainable fish production and processing* (pp. 259–291). Elsevier.

Semenova, A. A., Nasonova, V. V., & Tunieva, E. K. (2019). The effect of essential oils on the color stability of minced meat. *IOP Conference Series: Earth and Environmental Science, 333*(1), Article 012098. https://doi.org/10.1088/1755-1315/333/1/012098

Sengupta, A., Ghosh, M., & Bhattacharyya, D. (2015). In vitro antioxidant assay of medium chain fatty acid rich rice bran oil in comparison to native rice bran oil. *Journal of Food Science and Technology, 52*, 5188–5195. https://doi.org/10.1007/s13197-014-1543-z

Shahidi, F., & Wanasundara, U. N. (2002). Methods for measuring oxidative rancidity in fats and oils. In *Food lipids* (pp. 484–507). CRC Press.

Singh, A., Benjakul, S., & Prodpran, T. (2019). Chitooligosaccharides from squid pen prepared using different enzymes: Characteristics and the effect on quality of surimi gel during refrigerated storage. *Food Production, Processing and Nutrition, 1*(1), 5. https://doi.org/10.1186/s43014-019-0005-4

Song, R., Li, W., Deng, S., Zhao, Y., & Tao, N. (2023). Assessment of lipid composition and eicosapentaenoic acid/docosahexaenoic acid bioavailability in fish oil obtained through different enrichment methods. *Frontiers in Nutrition, 10*. https://doi.org/10.3389/fnut.2023.1136490

Stanojevic, L. P., Marjanovic-Balaban, Z. R., Kalaba, V. D., Stanojevic, J. S., & Cvetkovic, D. J. (2016). Chemical composition, antioxidant and antimicrobial activity of chamomile flowers essential oil (*Matricaria chamomilla* L.). *Journal of Essential Oil Bearing Plants, 19*(8), 2017–2028. https://doi.org/10.1080/0972060X.2016.1224689

Takeungwongtrakul, S., & Benjakul, S. (2013). Oxidative stability of shrimp oil-in-water emulsions as affected by antioxidant incorporation. *International Aquatic Research, 5*(1), 14. https://doi.org/10.1186/2008-6970-5-14

Tsivelika, N., Sarrou, E., Gusheva, K., Pankou, C., Koutsos, T., Chatzopoulou, P., & Mavromatis, A. (2018). Phenotypic variation of wild chamomile (*Matricaria chamomilla* L.) populations and their evaluation for medicinally important essential oil. *Biochemical Systematics and Ecology, 80*, 21–28. https://doi.org/10.1016/j.bse.2018.06.001

Valgimigli, L. (2023). Lipid Peroxidation and Antioxidant Protection. *Biomolecules, 13*(9), 1291. https://doi.org/10.3390/biom13091291

WHO. (2021). Key technical issues of herbal medicines with reference to interaction with other medicines. Retrived from https://www.who.int/publications/i/item/9789240019140 Accessed July 5, 2024.

Wong, J., Tay, Y. X., & Yue, G. (2023). Developing predictive growth models for Asian seabass using four generations of data. *Aquaculture and Fisheries*. https://doi.org/10.1016/j.aaf.2023.08.010

Yadav, N., Shakya, P., Kumar, A., Gautam, R. D., Chauhan, R., Kumar, D., … Singh, S. (2022). Investigation on pollination approaches, reproductive biology and essential oil variation during floral development in German chamomile (Matricaria chamomilla L.). *Scientific Reports, 12*(1), 15285. https://doi.org/10.1038/s41598-022-19628-0

Yarnpakdee, S., Benjakul, S., & Kingwascharapong, P. (2015). Physico-chemical and gel properties of agar from Gracilaria tenuistipitata from the lake of Songkhla, Thailand. *Food Hydrocolloids, 51*, 217–226. https://doi.org/10.1016/j.foodhyd.2015.05.004

Yue, G. H., Wang, L., Yang, Z., Sun, F., Tay, Y. X., Wong, J., & Yeo, S. (2022). Genomic resources and their applications in aquaculture of Asian seabass (Lates calcarifer). *Reviews in Aquaculture, 15*(2), 853–871. https://doi.org/10.1111/raq.12764

Zhang, Q., Jia, S., Bai, Y., Zhou, X., & Ding, Y. (2021). Formation mechanisms of reactive carbonyl species from fatty acids in dry-cured fish during storage in the presence of free radicals. *Journal of Future Foods, 1*(2), 203–210. https://doi.org/10.1016/j.jfutfo.2022.01.010